

INSTITUTE OF HIGH ENERGY PHYSICS, SERPUKHOV  
Report IFVE SKU 70-90

CERN LIBRARIES, GENEVA



CM-P00100683

DAMPING OF THE EFFECT OF THE INCREASE OF  
BEAM DIMENSIONS DUE TO THE INFLUENCE OF  
NON-LINEAR RESONANCES AT THE IHEP ACCELERATOR

V.I. Gridasov, K.P. Myznikov and V.N. Chepegin

Serpukhov 1970

Translated at CERN by A.T. Sanders

(Original: Russian)

Revised by N. Mouravieff

(CERN Trans. 71-30)

Geneva

May 1971

The emittance of the accelerated proton beam is one of the most important parameters determining the efficiency of the ejection system of the accelerator. However, even the first measurements made in the IHEP accelerator showed that beam emittance at the end of acceleration was considerably different from that calculated <sup>(1)</sup>. The purpose of the present work was to discover the reasons for this effect and to investigate experimentally into the possibility of eliminating it. Fig. 1 shows the dependence of the horizontal and vertical dimensions of the accelerated beam on the value of the magnetic field of the accelerator. The beam dimensions were determined by means of internal targets. The target was introduced into the beam at a given moment of the accelerating cycle. Its position could be varied vertically and horizontally with an accuracy of  $\pm 1$  mm. The edge of the beam corresponded to the target position for which no limitation of the intensity of the accelerated beam was observed through the pick-up electrodes with an accuracy of a few per cent. It can be seen from Fig. 1 that, beginning with a field of 9 k. oe, when noticeable iron saturation effects appear, the beam can be observed to increase in size in both planes. The character of the dependence (Fig. 1) then varies if the radial position of the accelerated beam is changed by selecting a corresponding frequency law for the accelerating voltage. In order to explain this effect, the dependence of the frequencies of the betatron oscillations on the radial position of the beam was measured <sup>(2)</sup> for various values of the magnetic field of the accelerator. Fig. 2 shows the dependences, plotted on the basis of these measurements, of the position of the lines of adjacent resonances in the accelerating process. The position of the beam upon acceleration for the two cases considered (Fig. 1) is shown by dotted lines. The y axis shows the position of the mean radius of the accelerated beam in relation to the central orbit and the corresponding frequency shift of the accelerating voltage.

By analysing Fig. 2 one can understand the character of the curves of Fig. 1. The increase in the beam dimensions at the end of acceleration is explained by the action of non-linear

resonances. Depending on the radius at which the beam is accelerated, the action of these resonances begins at different moments of the accelerating cycle. By comparing the curves in Fig. 1, measured in the central radius and for  $\langle \Delta R \rangle = -10$  cm, it can be observed that in both cases the beam for fields of over 9 k oe undergoes the action of third order resonances  $3Q_z = 29$  and  $2Q_z + Q_r = 29$ . In the first case their effect begins somewhat earlier; moreover, in the central radius at the end of acceleration the beam is subjected in addition to the action of a strong resonance  $3Q_r = 29$ .

The beam dimensions during the flat top of the magnetic cycle depending on the radial position of the beam were also investigated. The results are given in Fig. 3. They also can be explained on the basis of Fig. 2. When the beam position is near the central orbit its dimensions increase under the action of non-linear resonances. When the beam shifts outwards or inwards from the central orbit by more than 2 cm the parametric resonances also begin to act and the beam dimensions increase sharply.

Thus, the main reason for the increase of the beam dimensions at the end of the acceleration is the effect of non-linear resonances, the lines of which intersect in the acceleration process. Fig. 4 shows the working grid of the frequencies  $Q_{r,z}$ , and lines 1-6 show how the frequencies change when the beam shifts radially for different inductions. By comparing the phase trajectories (aa, bb, cc) corresponding to acceleration at different radii one can reach the conclusion that the shortest of them corresponds to the central radius. However even in this case the phase curve for different inductions intersects a large number of resonance lines. In order to exclude the action of the resonances, conditions were created in which for the whole duration of the acceleration the working point was in a square free from resonances. For this purpose, by choosing a strictly determined frequency variation law for the accelerating voltage, the beam, from 4 k. oe onwards was accelerated with an accuracy of  $\pm 1$  mm in the central radius. For

this beam position a current variation law in the gradient-correct poleface windings was chosen for which the trajectory of motion of the working point in the frequency grid corresponded to the curve AB (Fig. 4). The results of the measurement of the beam dimensions in this case are given in Fig. 5. It can be seen that the effect of the non-linear resonances is practically eliminated and consequently the beam dimensions decrease until the end of acceleration. The increase in the beam dimensions taking place throughout the flat top of the magnetic cycle was also eliminated. Fig. 6 (curves 1a,b) gives the dependence of the number of particles striking the target when it is in a different position in relation to the centre of the beam at the end of the flat top in the absence of gradient correction. Curves 2a,b show how these dependences change when the correction is switched on. The following conclusions can be reached on the basis of the experiments carried out:

1. A radial beam shift at the end of the accelerating cycle is highly undesirable, since the number of intersecting lines of non-linear resonances inevitably increases and the beam dimensions increase.
2. The most effective way of eliminating the action of the resonances is to stabilize the radial position of the accelerated beam and choose for the given radius the necessary gradient correction law for the duration of the acceleration. One can thus avoid an increase in the beam dimensions in the accelerating process and obtain values of the horizontal and vertical emittances not exceeding  $\pi$  mm/mrad.
3. The correcting regime studied makes it possible to improve the time structure of the beams of secondary particles generated on the internal targets, which appear owing to the effect of resonances when the accelerated beam is aimed at the target, and to increase the efficiency of the interaction between the accelerated beam and the target.

4. For fast and slow ejection the correcting regime studied is also highly effective, since it makes it possible considerably to reduce beam emittance and increase the efficiency of ejection. For slow ejection the correcting method studied can be successfully combined with the necessary correction of the quadratic non-linearity of the magnetic field<sup>4)</sup>.

In conclusion the writers wish to thank A. A. Kardash , V. V. Lapin and V. G. Sinenko, who were responsible for operating the gradient-correcting system when the experiments were carried out.

R e f e r e n c e s

1. V.I. Gridasov, A.A. Kardash et al. Methods of generating secondary particles on the internal targets of the IHEP accelerator. Proceedings of the VIIth International Conference on Accelerators. Armenian SSR Press, Vol. 1, 509, Erevan, 1970.
2. K.F. Gertsev, V.I. Gridasov et al. IHEP Preprint 70-86, Serpukhov, 1970.
3. V.I. Gridasov, A.A. Kardash et al. IHEP Preprint 70-57, Serpukhov, 1970.
4. K.P. Myznikov, V.M. Tatarenko, Yu. S. Fedotov. IHEP Preprint 70-51, Serpukhov, 1970.

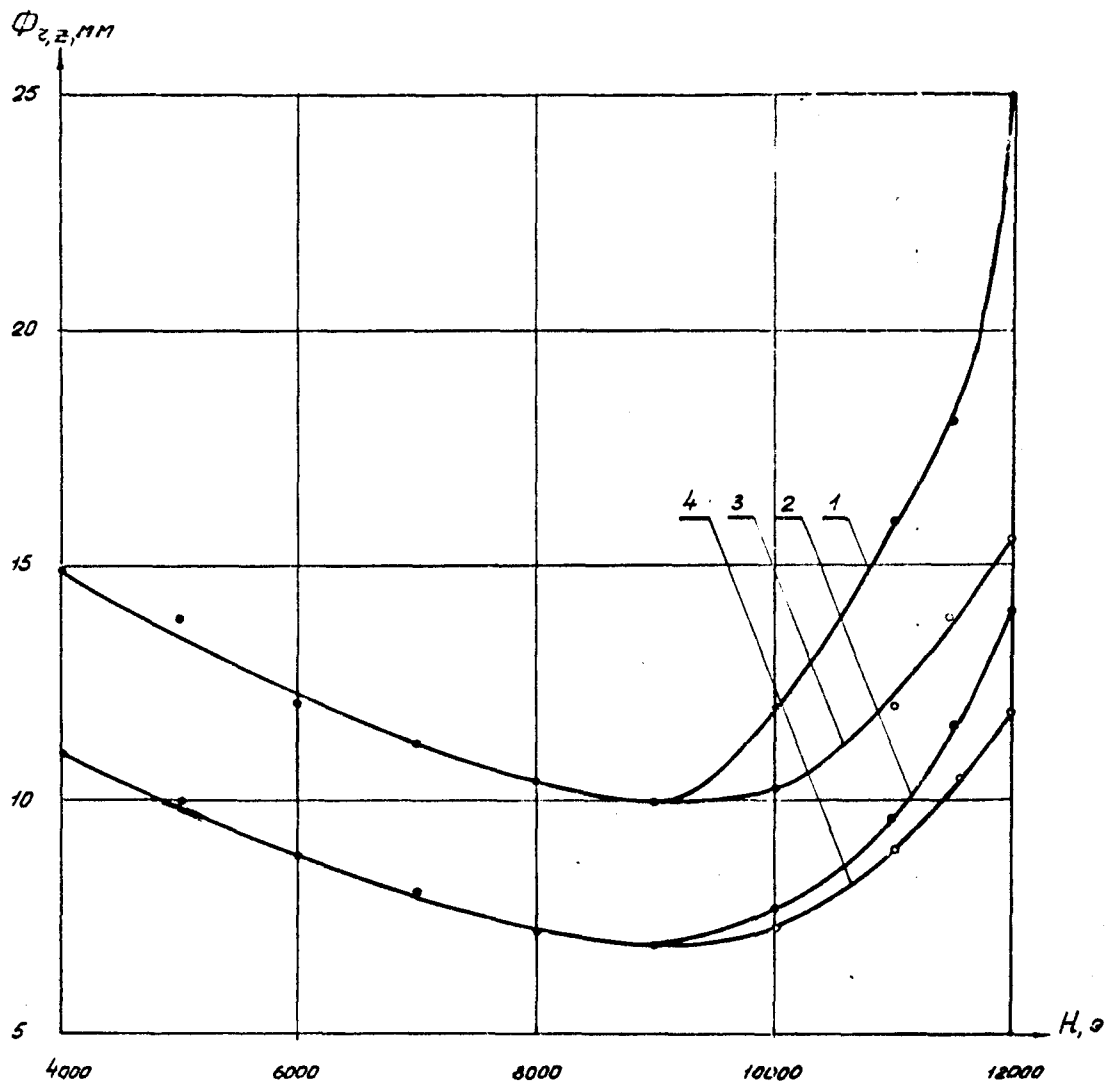


**Figure 1:** Dependence of the horizontal (Curves 1, 3) and vertical (Curves 2, 4) dimensions of the beam on the value of the magnetic field of the accelerator in the central (Curves 1, 2) and "natural" (Curves 3, 4) radii ( $\langle \Delta R \rangle = -10$  mm).

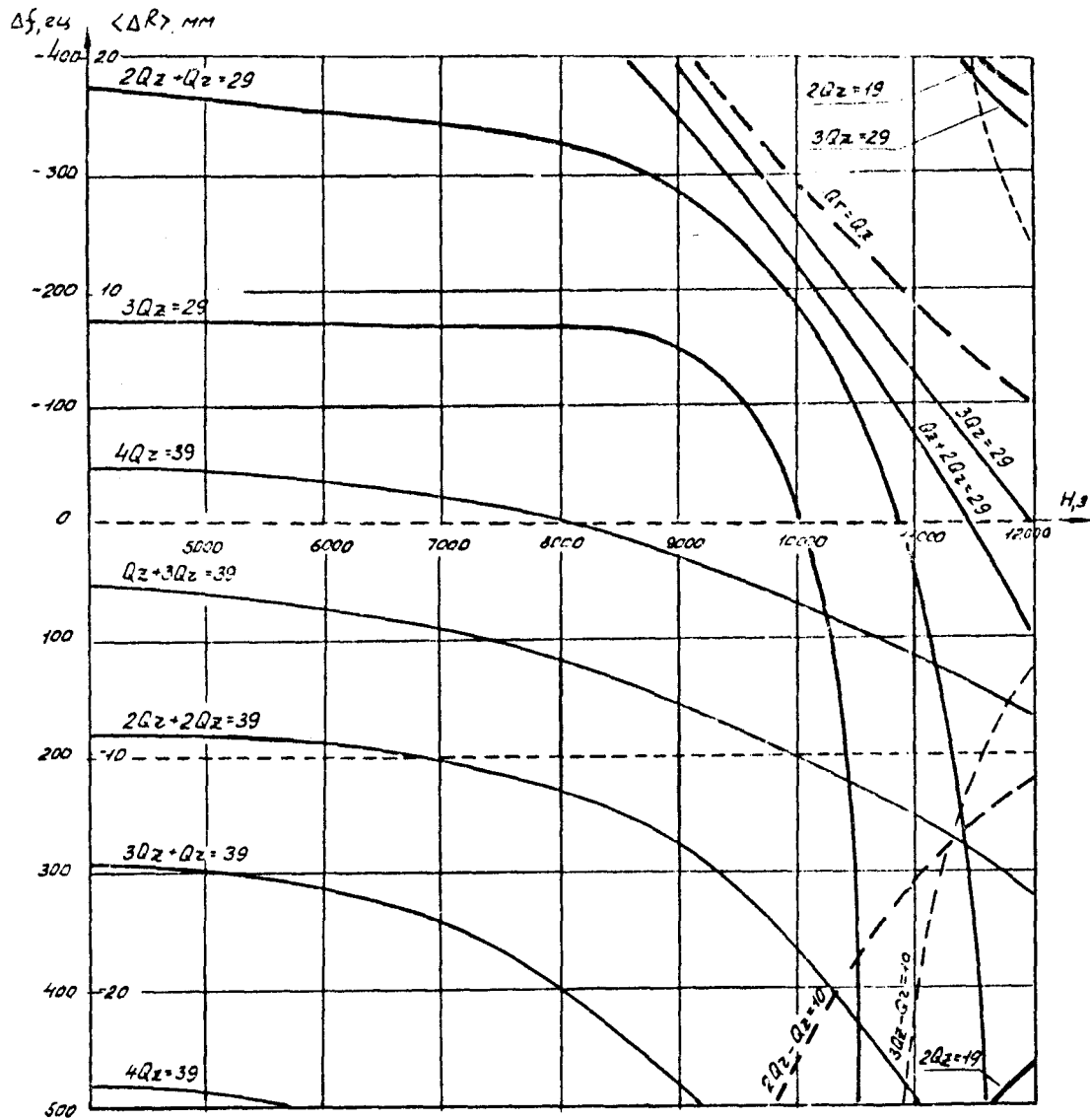


**Figure 2:** Trajectories of lines of adjacent resonances in the accelerating process. The y axis shows the position of the mean radius of the accelerated beam in relation to the central orbit and the corresponding frequency shift of the accelerating voltage.



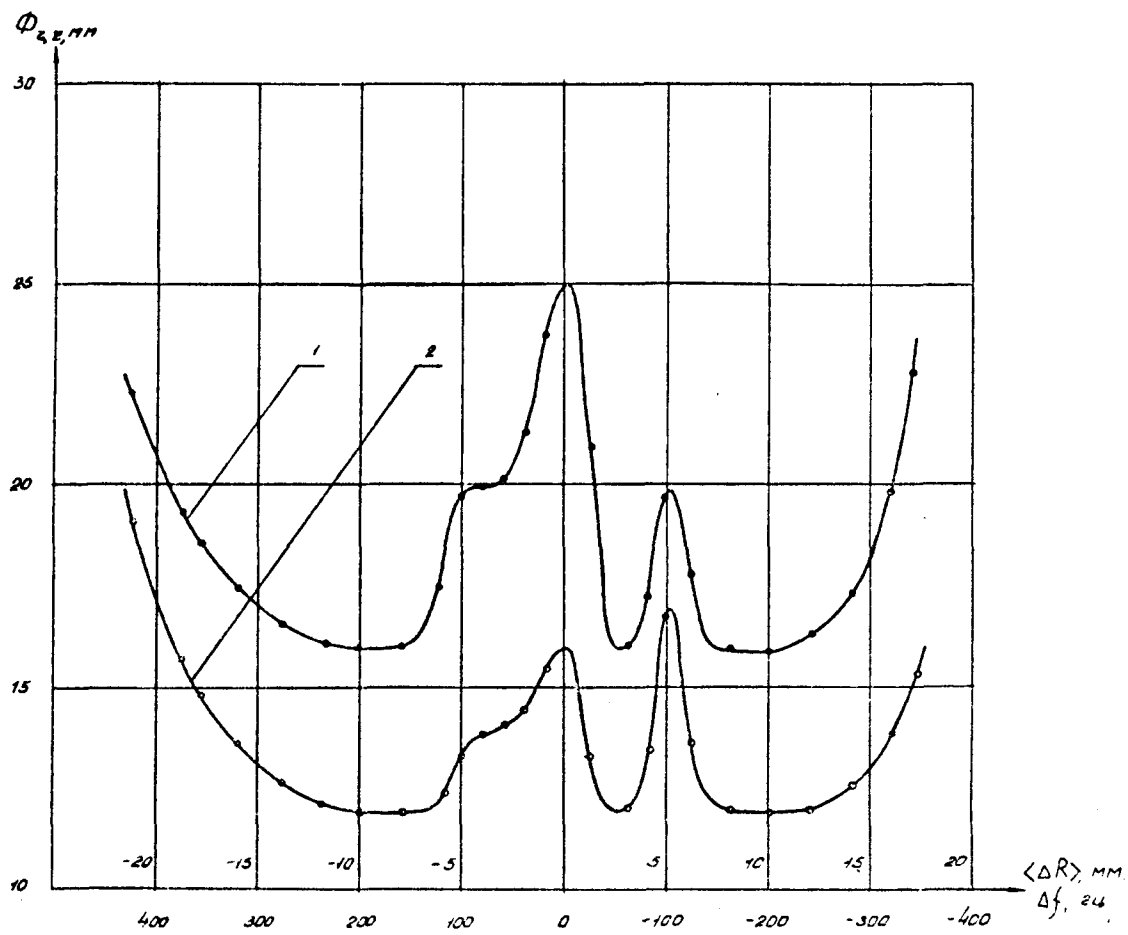


**Figure 3:** Dependence of the horizontal (Curve 1) and vertical (Curve 2) dimensions of the accelerated beam for its motion in different radii during the flat top of the magnetic field  $H = 12$  k. oe.

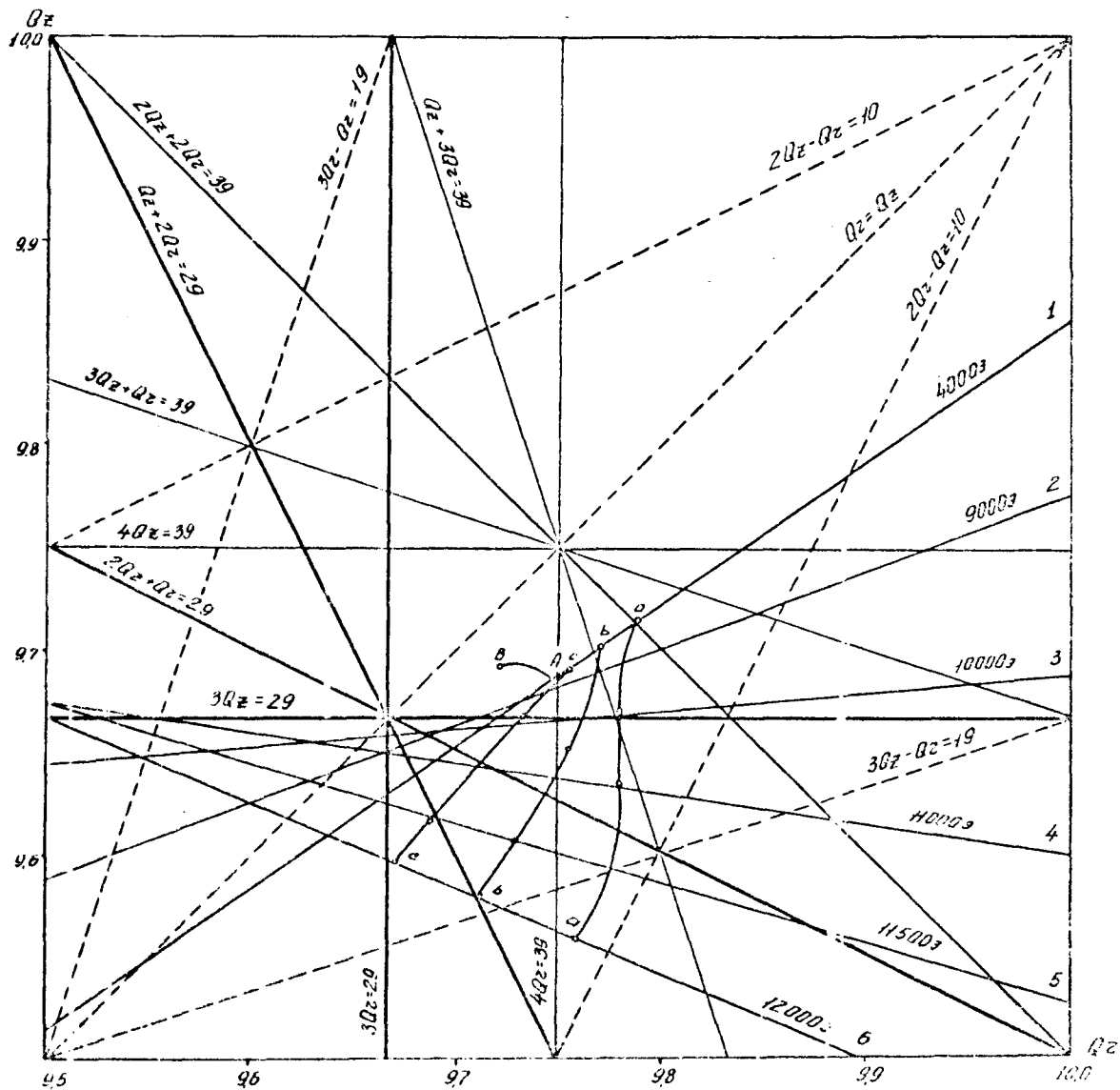


**Figure 4:** Working grid of the frequencies  $Q_1, Q_2$  with the lines of resonance up to the fourth order. Lines 1-6 are the trajectories of the working point for radial beam shift at different inductions; aa, bb, cc are the phase trajectories corresponding to acceleration at radii  $\langle \Delta R \rangle = -10$  mm,  $\langle \Delta R \rangle = -5$  mm,  $\langle \Delta R \rangle = 0$ , AB being the trajectory of the working point with gradient correction.

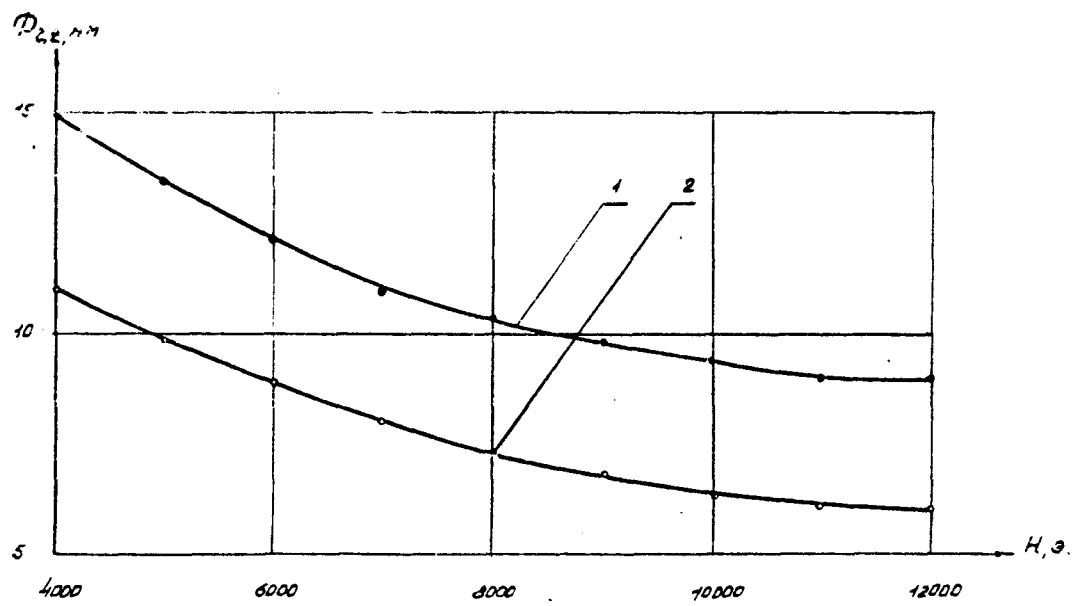


**Figure 5:** Dependence of the horizontal (Curve 1) and vertical (Curve 2) dimensions of the beam on the value of the magnetic field of the accelerator with acceleration in the central radius and gradient correction.

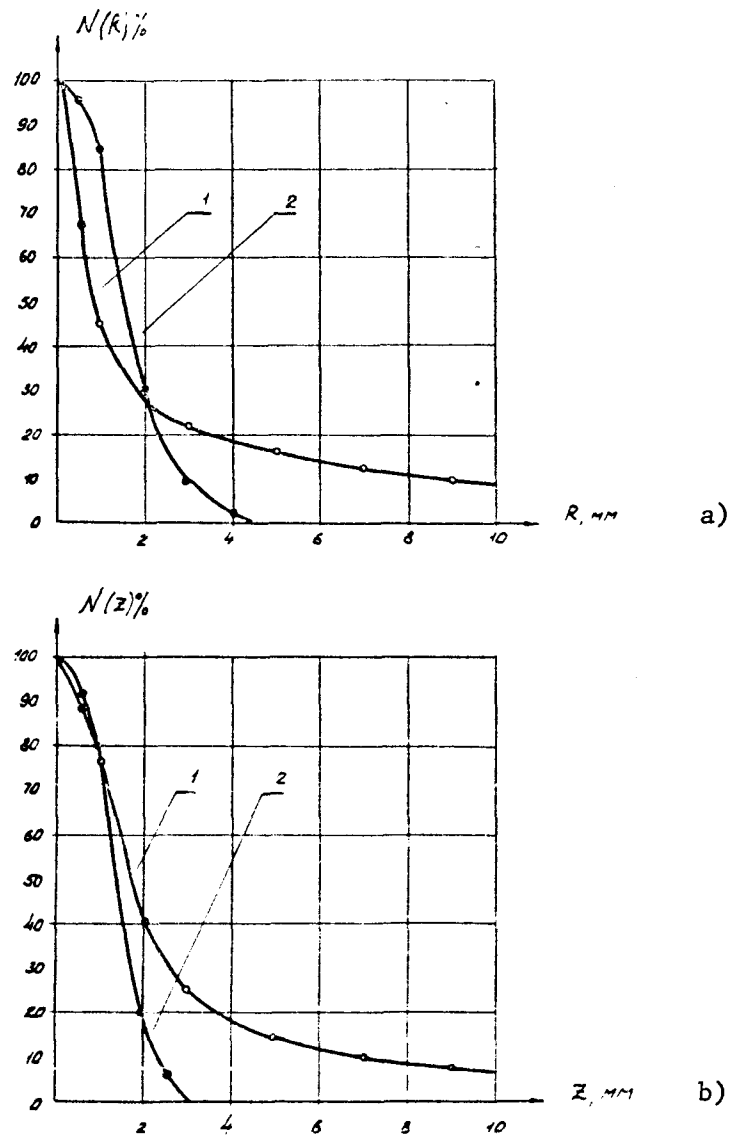


**Figure 6:** Dependence of the number of particles in the beam interacting with the target on the radial (Case a) and vertical (Case b) position of the target without gradient correction (Curves 1) and with gradient correction (Curves 2).